ERS-ENVISAT TANDEM CROSS - INTERFEROMETRY COHERENCE ESTIMATION

Urs Wegmüller, Maurizio Santoro, Charles Werner, Tazio Strozzi and Andreas Wiesmann

GAMMA Remote Sensing, Worbstrasse 225, 3073 Gümligen, Switzerland
tel: +41 31 951 7005, fax: +41 31 951 7008, e-mail:wegmuller@gamma-rs.ch

ABSTRACT

ERS-ENVISAT cross-interferometry is a unique tool for a number of applications since it combines a short repeat-pass interval (28 minutes) with a long perpendicular baseline (2 km). Temporal decorrelation effects are limited and the sensitivity to topographic features is strongly enhanced. In this contribution the focus is on problems encountered during the coherence estimation in ERS-ENVISAT cross-interferometry. Because of the ERS-2 Doppler Centroid variations the azimuth common band available is often only a relatively small fraction of the PRF. Similarly, in the case of not ideal baselines, the common range bandwidth is often much smaller than the chirp bandwidth. Furthermore, high phase gradients in the cross-interferograms can significantly affect the coherence estimates. In our contribution we propose methodologies to reduce these problems in the coherence estimation.

Index Terms— ERS, ENVISAT, cross-interferometry, coherence estimation, split-beam interferometry

1. INTRODUCTION

In 2002 ESA launched the ENVISAT satellite with the Advanced SAR (ASAR). The ENVISAT is operated in the same orbits as the ERS-2, preceding ERS-2 by approximately 28 *minutes*. One of the ASAR modes, namely IS2 at VV-polarization corresponds closely to the ERS-2 mode, except for the slightly different sensor frequency used. A unique opportunity offered by these two similar SAR instruments operated in the same orbital configuration is ERS-2 – ENVISAT cross-interferometry (CInSAR). The almost simultaneous acquisition of SAR images by ERS-2 and ENVISAT allows the generation of an interferogram characterized by a short 28 *minutes* repeat-pass interval. However, because of the slightly different sensor frequency, cross-interferograms show coherence only under particular conditions. Besides the requirement concerning an at least partial Doppler spectra overlap, only at perpendicular baselines of approximately 2 *kilometers* can the look-angle effect on the reflectivity spectrum compensate for the carrier frequency difference effect. Given the large baseline and short time interval ERS-ENVISAT CInSAR has a good potential, e.g. for the generation of precise digital elevation models (DEMs) in relatively flat areas [1,2]. There is interest in such DEMs e.g. in coastal zones with low relief, river plains, and wetlands, in particular at high latitudes where the SRTM DEM is not available [3].

Between 2002 and mid 2007 only very few adequate ERS-2 ENVISAT pairs were acquired. To support further investigation of ERS-2 - ASAR CInSAR ESA operated ERS-2 and ENVISAT for certain time periods as a constellation in carefully controlled orbits during so-called ERS-2 - ENVISAT Tandem (EET) Campaigns. A first EET Campaign was between 27 September 2007 and 12 February 2008. A second one took place in late 2008 early 2009 and a third one may be conducted in late 2009. During the first two EET Campaigns, the nominal perpendicular baseline for mid to high northern latitudes was 2*km* with ERS-2 observing the area at a slightly higher incidence angle than ENVISAT, to compensate the slight difference in the carrier frequencies between the two instruments.

In this contribution the focus is on the estimation of coherence in areas with high phase gradients. Analyzing a significant number of EET pairs revealed some problems with the coherence estimation. Concerning the interpretation of coherence values there are two main uses, one is that the coherence is a measure for the phase noise of the interferogram, so it is used as a quality measure in interferometry. The other use is that the coherence is a target characteristic. It is clear that this value may depend on the radar frequency and the incidence angle used, but ideally it should be independent of parameters as the range and azimuth bandwidth used.

In the case of EET CInSAR we noticed two particular problems with the coherence estimation. The first concerned the very high phase gradients between adjacent pixels in the case of surfaces which are not perfectly flat. At a 2*km* baseline the height ambiguity is in the order of 5m per phase cycle. So 5m height will cause already a full fringe (phase cycle) and this may occur over very few pixels. Similarly, available DEMs such as the SRTM DEM may have an accuracy in this order. The "height noise" of the SRTM DEM will cause significant local phase variation in the differntial interferogram which will significantly decrease the coherence estimated. The second problem found was that the range and azimuth common band filtering applied in EET CInSAR quite often reduces the bandwidth used to a relatively small fraction of the initially available bandwidth. How this filtering is done and how the coherence is

Table 1. CInSAR characteristics of ERS – ENVISAT pairs over Franz Josef Land (81.0 deg. N, 61.0 deg E). $B_\perp$ stands for the perpendicular baseline component, dDC for the difference between the Doppler Centroid of the ERS-2 and the ENVISAT ASAR scenes, and dh for the height ambiguity.

Site	Date	$B_\perp$ [*m*]	dDC [*Hz*]	dh [*m*]
Franz Josef Land	20070928	2047	650	4.60
Franz Josef Land	20071207	2066	550	4.56

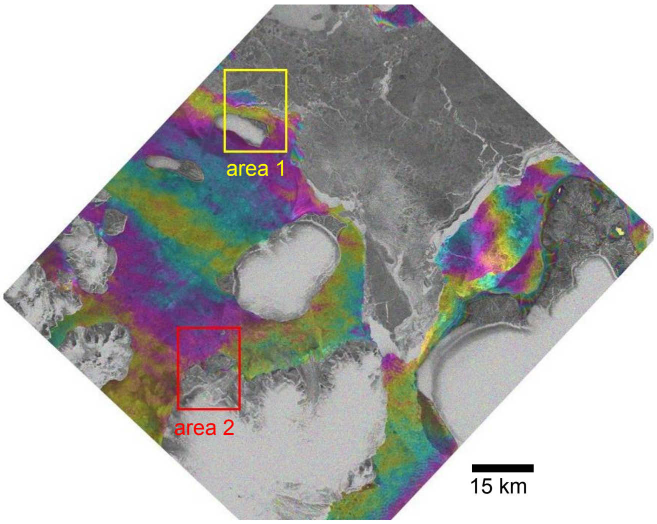

Figure 1 Geocoded EET cross-interferogram over Franz Josef Land, 7-Dec-2007. Yellow and red boxes indicate areas 1 and 2.

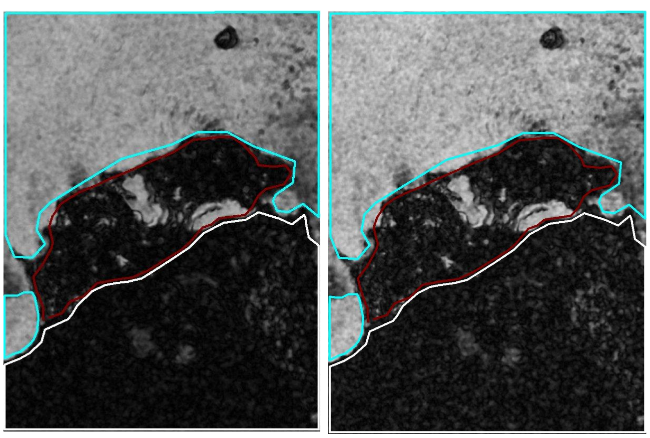

Figure 2 Geocoded EET CInSAR coherence estimates over Franz Josef Land (area 2 shown in Figure 1) on 7-Dec-2007 using 50% azimuth bandwidth (left) and 25% azimuth bandwidth (right) using a linear gray scale between 0.0 and 1.0. Area size 15km x 20km.

estimated can significantly influence the estimated coherence.

In the following we present possibilities to reduce the coherence dependence on the common bandwidth and high local phase gradients. This is done using two EET CInSAR pairs over Franz Josef Land with almost ideal perpendicular baselines (see Table 1). Figure 1 shows the EET cross interferogram on 7-Dec-2007. A significant fraction of the area is young sea ice. This area is flat and shows high coherence in areas where the sea ice doesn't move fast. Then there are land masses which are partly rock and partly covered by glaciers. At least the non-moving sea ice and the rock area are expected to have high coherence.

2. EET CINSAR COHERENCE ESTIMATION

2.1 Coherence estimation in the case of reduced bandwidths

Because of the significant variations in the ERS-2 Doppler Centroids azimuth common band filtering applied in EET CInSAR often reduces the azimuth bandwidth considered for the interferogram to a relatively small fraction of the PRF. Similarly, range common band filtering with a bandwidth significantly smaller than the chirp bandwidth is applied if the perpendicular baseline deviates significantly from 2km.

Our standard approach is to apply the azimuth and range band-pass filtering to the SLC while maintaining the range and azimuth pixel spacing. The number of equivalent looks per pixel falls significantly below 1. In the coherence estimation it is assumed, though, that one SLC pixel corresponds to one look. As a result a somewhat too low coherence value is estimated.

The better approach is to reduce the spatial sampling along with the resolution reduction from the band-pass filtering. In practice we do this without change to the SLC sampling, but by starting the coherence estimation not from the one-pixel interferogram but from the one-look interferogram. The one-look interferogram is obtained by multi-looking of the one-pixel differential interferogram. The coherence estimation starts then from the single-look interferogram after setting the coherence of the individual pixels in the single-look interferogram to 1.0. Figure 2 shows the coherence estimated with this methodology over area 2 shown in Figure 1 using 50% azimuth bandwidth (left) which corresponds to the full overlapping bandwidth available and 25% azimuth bandwidth (right). The three main surface classes young sea ice (blue polygon), rock area (brown) and land ice (white) are roughly delineated to facilitate the interpretation. Comparable coherence estimates are obtained. The main disadvantages of the reduced bandwidth based estimation are an increased noise in the coherence estimation as well as an increased bias observed at low coherence levels. This is expected because a smaller number of looks was considered in the coherence estimation.

2.2 Coherence estimation in areas with very high phase gradients

In areas with very high phase gradients too low coherences are typically estimated because it is not possible to reliably subtract the strongly varying interferometric phase. In the case of EET CInSAR this problem occurs if the topographic phase is not sufficiently well modeled, which is very often the case. Considering the height ambiguity in the order of 5m means that meter accuracy is required for the DEM used to simulate the topographic phase. Such accurate

DEMs are very often not available. For our processing over Franz Josef Land we used a constant height reference as we had no DEM available. The coherence estimates in Figure 2 show very low coherence over most the rock area because of the present high phase gradients.

The methodology proposed to improve the coherence estimation in such a case is to consider a "split-beam" interferogram. The term "split-beam" is used because the radar signals are split into two beams with slightly different aspect angles. "Split-beam" interferograms were used in the past to estimate displacements along the azimuth direction [4]. For the coherence estimation the advantage of the split-beam interferogram is that there is very little phase change. Only very fast displacements in azimuth direction will cause a noticeable phase change. So the split-beam interferogram shows basically a constant phase affected only by the present phase noise.

The processing sequence used is as follows. The available azimuth bandwidth (about 50% in the case of the EET pair on 7-Dec-2007) is divided in two non-overlapping azimuth bands of equal width. This is done for both SLCs of the EET pair by band-pass filtering. For both pairs of sub-band SLCs one-pixel interferograms are calculated. The combined interferogram is then calculated from the one-pixel interferograms by multiplication of one complex interferogram with the complex conjugate of the other interferogram. The resulting phase corresponds to the phase of the "split-window" interferogram. An initial multi-looking is then applied to move from the one-pixel geometry to a one-look geometry. Starting from the one-look split-beam interferogram the coherence is estimated.

Figure 3 shows phase and estimated coherence of the split-beam interferogram. Except for phase noise the phase of the split-beam interferogram appears constant (blue color corresponds to 0.0 radian), this even over the rock area in the image center characterized by significant variations of the topography and very high phase gradients in the normal EET cross interferogram. While similar coherence values are estimated over the stable flat sea-ice area we observe much higher values over the rock area, confirming the potential of this methodology to discriminate this stable "high coherence target" from decorrelating targets as the land ice (probably decorrelated at this long baseline due to the importance of volume scattering). The same methodology was also applied to the September 2007 EET pair over the same area. The results shown in Figure 4 confirm the findings. In September there was no stable sea-ice formed, so that most of the area shows very low coherence, with the exception of the rock area.

3. SPLIT-BEAM INTERFEROGRAM PHASE

The main reason to generate a split-beam interferogram was to get an interferogram with much lower phase variation to get better coherence estimates in areas with high phase gradients in the conventional differential interferogram.

Calculating the split-beam interferogram it is worth-while

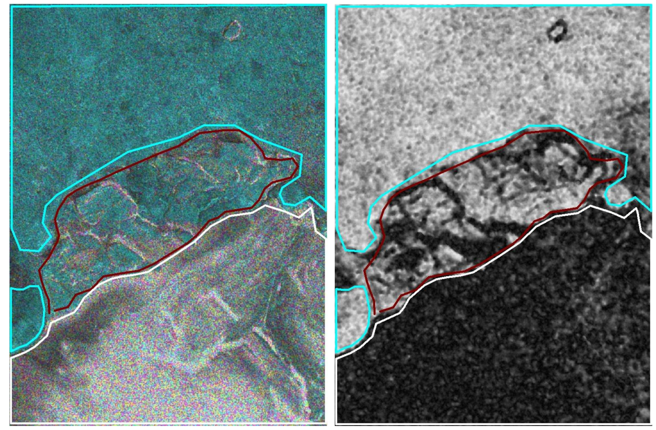

Figure 3 Geocoded EET phase (left, color cycle corresponding to phase cycle) and coherence estimate (right) of split-beam interferogram on 7-Dec-2007 over Franz Josef Land (area 2 shown in Figure 1).

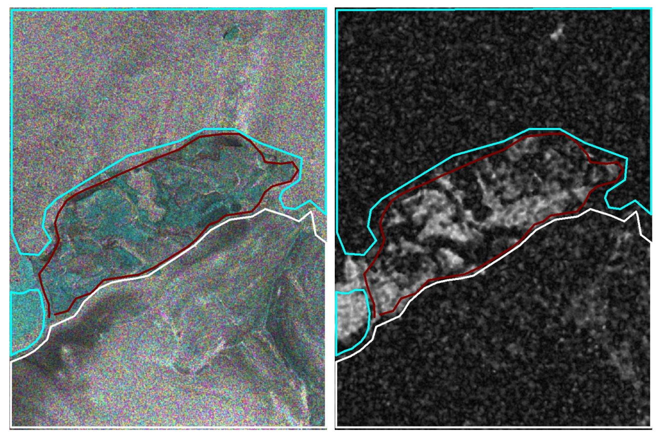

Figure 4 Geocoded EET phase (left) and coherence estimate (right) of split-beam interferogram on 28-Sep-2007 over Franz Josef Land (area 2 shown in Figure 1).

considering also the phase of the split-beam interferogram. As derived in [4] the phase ϕ of the split-beam interferogram can be approximated for small squint angles by

$$\phi = \frac{2\pi d_{az}}{l} \qquad (1)$$

with d_{az} the displacement in azimuth direction and l the antenna size (about 10m for ERS-2 and ENVISAT ASAR). The relation between phase noise σ_ϕ, signal to noise ratio (*SNR*) and coherence γ can be approximated by [5]

$$\sigma_\phi = \frac{1}{\sqrt{2N_L}} \frac{\sqrt{1-\gamma^2}}{\gamma} \quad \text{with} \quad \gamma = \frac{\gamma_{spatial,temporal}}{1+SNR^{-1}} \qquad (2)$$

In the case of fast coherent displacements along the azimuth direction a non-zero phase is observed. In the data over Franz Josef Land this is the case over some fast moving sea-ice. Figure 5 shows the split-beam interferogram phase and coherence for the 7-Dec-2007 EET pair over Franz Josef Land, area 1. The observed phase in the North-Western corner corresponds to fast motion as is confirmed by the offset tracking result shown in Figure 6 [6].

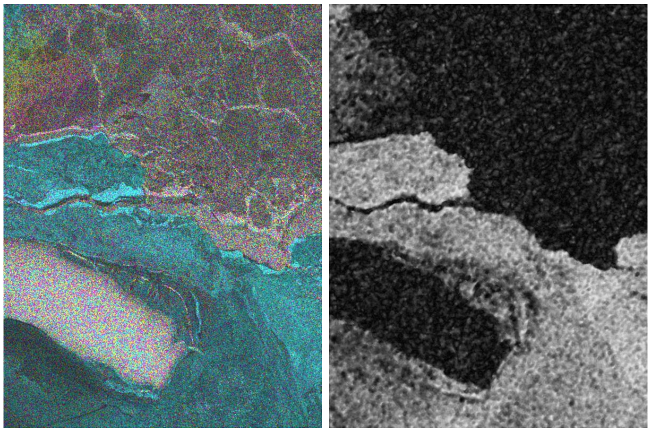

Figure 5 Geocoded EET phase (left) and coherence estimate (right) of split-beam interferogram on 7-Dec-2007 over Franz Josef Land (area 1 shown in Figure 1).

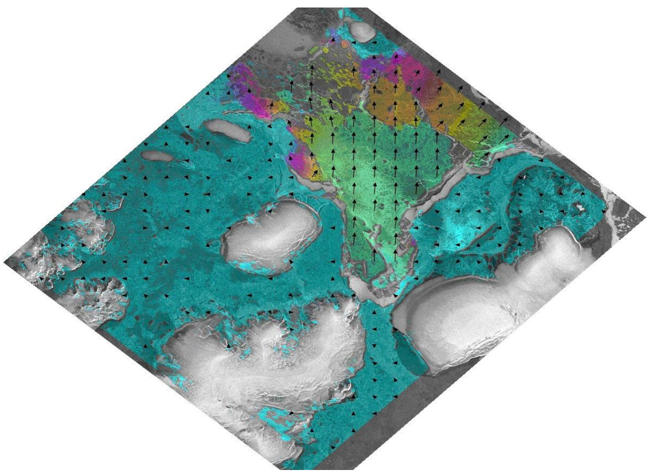

Figure 6 Geocoded sea ice displacement map derived from a 28' ERS-ENVISAT pair acquired on 7-Dec-2007 over Franz Josef Land (area size 53km x 56km). The image brightness corresponds to the backscattering of the ASAR image. For more discussion on this result and the methodology used see [6].

4. DISCUSSION

Working with reduced band-width interferograms showed that some aspects need to be taken into account which have typically been ignored so far. The coherence estimation needs to be adapted for band-pass filtered interferograms because one filtered SLC pixel does not correspond to one equivalent look. This is very relevant when using ERS-2 zero gyro-mode acquisitions because of the strong temporal variation of the Doppler Centroids values over a given area of interest. A simple procedure for a more adequate coherence estimation has been proposed and the results obtained confirm the potential.

For the other problem addressed, the coherence estimation in areas with high phase gradients, the split-beam procedure proposed demonstrated a good potential to improve the estimation over the standard procedure used. In rock areas with significant topographic phase variations the split-beam methodology estimated significantly higher coherence values than the standard methodology. It was clearly possible based on the coherence to discriminate between the rock area and open water.

Decorrelation effects also very relevant in EET CInSAR include imperfect range common band filtering in the case of varying slopes and non-overlapping range spectra for steeper slopes. Geometric decorrelation is expected to be relevant in the case of the land ice because of the long baseline and the significant penetration of the microwaves into the ice. Finally, for fast moving sea ice temporal change and imperfect co-registration reduces the coherence.

5. CONCLUSIONS

In this paper we presented coherence estimation methodologies that help to reduce the problems encountered in the case of significantly band-pass filtered scenes and for areas with very high phase gradients. While the conventional coherence estimation method showed in two EET CInSAR pairs very low coherence values over a rock area with varying topography significantly hgher values were obtained using the split-beam coherence estimation methodology.

The results confirm a relatively good potential of the proposed methodologies. Further work, including more examples and a more thorough theoretical background, should follow to consolidate these methods.

6. ACKNOWLEDGMENTS

This work was supported by ESA under contract 19366/05/I-EC–CCN5 and the project "ERS-ENVISAT Tandem Cross-InSAR Campaigns: Case Studies". ERS and ENVISAT data are copyright ESA and were received through CAT1 AO Project 4901.

7. REFERENCES

[1] M. Santoro, J. I. H. Askne, U. Wegmüller, and C. L. Werner, "Observations, modeling, and applications of ERS-ENVISAT coherence over land surfaces," IEEE Trans. Geosci. Remote Sensing, vol. 45, pp. 2600-2611, 2007.

[2] U. Wegmüller, M. Santoro, C. Werner, T. Strozzi, A. Wiesmann, W. Lengert, and N. Miranda, "ERS-2 Zero-Gyro-Mode data application showcases," *Proc. Fringe 2007 Workshop*, ESA-ESRIN, Frascati, 26-30 November, 2007.

[3] B. Rabus, M. Eineder, A. Roth, and R. Bamler, "The shuttle radar topograpy mission - a new class of digital elevation models acquired by spaceborne SAR," *ISPRS Journal of Photogrammetry & Remote Sensing*, vol. 57, pp. 241-262, 2003.

[4] N. B. D. Bechor and H. Zebker, "Measuring two-dimensional movements using a single InSAR pair", Geophysical Research Letters, Vol. 33, L16311, doi:10.1029/2006GL026883, 2006.

[5] E. Rodriguez and J. M. Martin, "Theory and design of interferometric synthetic aperture radars", IEE Proc. Part F Radar Signal Process, 139(2), 149-159, 1992.

[6] Santoro M., U. Wegmüller, T. Strozzi, C. Werner, A. Wiesmann and W. Lengert, "Thematic applications of ERS-ENVISAT cross-interferometry", Proc. IGARSS'08, Boston, 6-11 Jul. 2008.